

1 **Big data managing in a landslide Early Warning System: experience from a ground-based**  
2 **interferometric radar application**

3 Emanuele Intrieri<sup>1</sup>, Federica Bardi<sup>1</sup>, Riccardo Fanti<sup>1</sup>, Giovanni Gigli<sup>1</sup>, Francesco Fidolini<sup>2</sup>, Nicola  
4 Casagli<sup>1</sup>, Sandra Costanzo<sup>3</sup>, Antonio Raffo<sup>3</sup>, Giuseppe Di Massa<sup>3</sup>, Giovanna Capparelli<sup>3</sup>, Pasquale  
5 Versace<sup>3</sup>.

6 <sup>1</sup> Department of Earth Sciences, University of Florence, via La Pira 4, 50121, Florence, Italy

7 <sup>2</sup> Pizzi Terra srl, via di Ripoli 207H, 50126, Florence, Italy

8 <sup>3</sup> Department of Computer Engineering, Modelling, Electronics and Systemics, University of  
9 Calabria, Ponte Pietro Bucci, Cube 41b, 87036, Arcavacata di Rende (CS), Italy

10

11 *Correspondence to:* Emanuele Intrieri (emanuele.intrieri@unifi.it)

12

13

14 **Keywords:** early warning system; slope instability; big data; monitoring; landslide; risk  
15 management; ground-based interferometric radar

16

17 **1 Abstract**

18 A big challenge in terms of landslide risk mitigation is represented by the increasing of the  
19 resiliency of society exposed to the risk. Among the possible strategies to reach this goal, there is  
20 the implementation of early warning systems. This paper describes a procedure to improve early  
21 warning activities in areas affected by high landslide risk, such as those classified as Critical  
22 Infrastructures for their central role in society.

23 This research is part of the project “LEWIS (Landslides Early Warning Integrated System): An  
24 Integrated System for Landslide Monitoring, Early Warning and Risk Mitigation along Lifelines”.

25 LEWIS is composed of a susceptibility assessment methodology providing information for single  
26 points and areal monitoring systems, a data transmission network and a Data Collecting and  
27 Processing Center (DCPC), where readings from all monitoring systems and mathematical models  
28 converge and which sets the basis for warning and intervention activities.

29 The aim of this paper is to show how logistic issues linked to advanced monitoring techniques such  
30 as big data transfer and storing, can be dealt with, compatibly with an early warning system.  
31 Therefore, we focus on the interaction between an areal monitoring tool (a ground-based  
32 interferometric radar) and the DCPC. By converting complex data into ASCII strings and through  
33 appropriate data cropping and average, and by implementing an algorithm for line of sight  
34 correction, we managed to reduce the data daily output without compromising the capability of  
35 performing.

36

## 37 **2 Introduction**

38 Urbanization, especially in mountain areas, can be considered a major cause for high landslide risk  
39 because of the increased exposure of elements at risk. Among the elements at risk, important  
40 communication routes, such as highways, can be classified as Critical Infrastructures (CIs), since  
41 their rupture can cause chain effects with catastrophic damages on society (Geertsema et al 2009;  
42 Kadri et al. 2014). On the other hand, modern society is more and more dependent from CIs and  
43 their continuous efficiency (Lebaka et al., 2016), and this has risen their value over the years. The  
44 result is a higher social vulnerability in the face of loss of continuous operation (Kröger, 2008). The  
45 main objective was to improve the social preparedness to the growing landslide risk, according with  
46 the suggestions of several authors (Gene Corley et al., 1998; Baldrige et al., 2011; Urlainis et al.  
47 2014; 2015). This led to the development of several approaches and frameworks for increasing the  
48 resiliency of society exposed to the risk (Kröger, 2008; Cagno et al., 2011 and references therein).  
49 The resiliency policy of course involves prevention activities but also, and more importantly, those  
50 activities needed to maintain functionality after disruption (Snyder and Burns, 2009) and to  
51 promptly alert incoming catastrophes in order to protect people and prepare for a possible damaging  
52 of the endangered CI. Among these activities, the implementation of integrated landslides early  
53 warning systems (*i.e.* LEWIS, Versace et al., 2012; Costanzo et al., 2016) reveals its increasing  
54 importance.

55 In this context, the methodology described in this paper has been conceived; it has been tested and  
56 validated on a portion of an Italian highway, affected by landslides and selected as case study: it is  
57 located in Southern Italy, along a section of the A16 highway, an important communication route  
58 that connects Naples to Bari where a Ground-Based Interferometric Synthetic Aperture Radar (GB-  
59 InSAR) has been installed on the test site, in order to obtain spatial monitoring data.

60 One of the main drawbacks of advanced instruments such as GB-InSAR is how to handle the large  
61 data flow deriving from continuous real-time monitoring. The issue is to reduce the capacity needed  
62 for analyzing, transmitting and storing big data without losing important information. The main  
63 feature of this paper is indeed the management of monitoring data in order to filter, correct, transfer  
64 and access them compatibly with the needs of an early warning system.

65

## 66 **3 Materials and methods**

### 67 *3.1 GB-InSAR*

68 The GB-InSAR is composed of a microwave transceiver mounted on a linear rail (Tarchi et al.,  
69 1997; Rudolf et al., 1999; Tarchi et al., 1999). The system used is based on a Continuous Wave –  
70 Stepped Frequency radar, which moves along the rail at millimeter steps, in order to perform the  
71 synthetic aperture; the longer the rail the higher the cross-range resolution. The microwave  
72 transmitter produces, step-by-step, continuous waves around a central frequency, which influences  
73 the cross-range resolution and determines the interferometric sensitivity *i.e.* the minimum  
74 measurable displacement, usually largely smaller than the corresponding wavelength.

75 The radar produces complex radar images containing the information relative to both phase and  
76 amplitude of the microwave signal backscattered by the target (Bamler and Hartl, 1998; Antonello

77 et al., 2004). The amplitude of a single image provides the radar reflectivity of the scenario at a  
78 given time, while the phase of a single image is not usable. The technique that enables to retrieve  
79 displacement information is called interferometry and requires the phase from two images. In this  
80 way, it is possible to elaborate a displacement map relative to the elapsed time between the two  
81 acquisitions.

82 The main added value of GB-InSAR is its capability of blending the boundary between mapping  
83 and monitoring, by computing 2D displacement maps in near real-time. The use of this tool to  
84 monitor structures, landslides, volcanoes, sinkholes is largely documented (Calvari et al., 2016; Di  
85 Traglia 2014; Intrieri et al., 2015; Bardi et al., 2016, 2017; Martino and Mazzanti, 2014; Severin,  
86 2014; Tapete et al., 2013), as well as for early warning and forecasting (Intrieri et al., 2012; Carlà et  
87 al., 2016a; 2016b; Lombardi et al., 2016).

88 GB-InSAR systems probably reveal their full potential in emergency conditions. They are  
89 transportable and only require from few tens of minutes to few hours to be installed (depending on  
90 the logistics of the site). Moreover, they can detect "near-real time" area displacements, without  
91 accessing the unstable area, 24h and in all weather conditions (Del Ventisette et al., 2011; Luzi,  
92 2010; Monserrat et al., 2014). On the other hand, some limitations reduce the GB-InSAR technique  
93 applicability: first of all the scenario must present specific characteristics in order to reflect  
94 microwave radiations, maintaining high coherence values (Luzi, 2010; Monserrat et al., 2014); only  
95 a component of the real displacement vector can be identified (i.e. the component parallel to the  
96 sensor's line of sight); maximum detectable velocities are connected to the time that the system  
97 needs to obtain two subsequent acquisitions. Sensors need power supply that, for long term  
98 monitoring, cannot be replaced by batteries, generators or solar panels.

99 With the specific aim of performing an early warning system, data acquired *in situ* must be sent  
100 automatically to a "control center" where they are integrated in a complete early warning system  
101 procedure (Intrieri et al., 2013). In this sense, another main limitation is represented by the necessity  
102 to transfer a high quantity of data, whose weight has to be reduced to the minimum, in order to  
103 reduce the load on transmission network.

104 The employed system is a portable device designed and implemented by the Joint Research Center  
105 (JRC) of the European Commission and its spin-off company Ellegi-LiSALab (Tarchi et al., 2003;  
106 Antonello et al., 2004).

### 107 3.2 Early warning system architecture

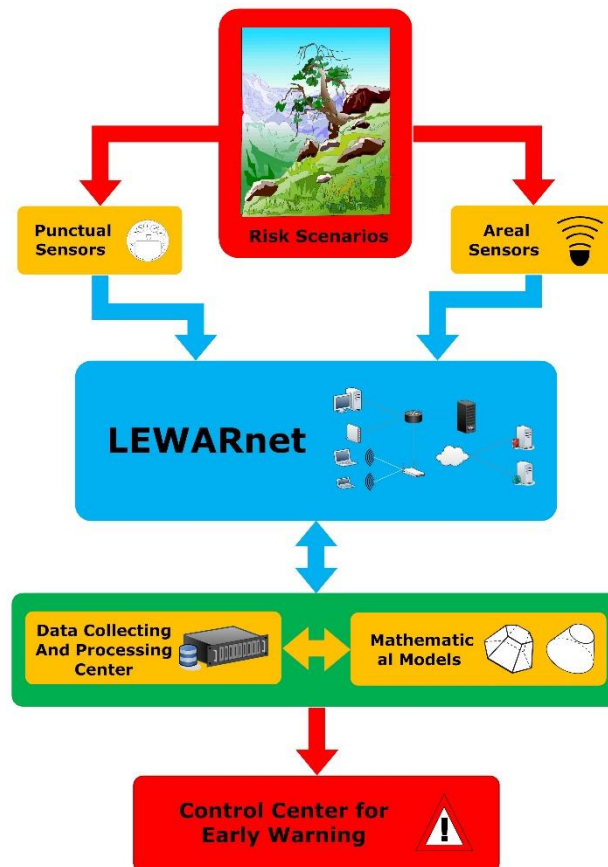
108 Morphological features, hydrogeological factors and sudden rainfall can cause diverse types of  
109 movements or fall of earthy and rock materials. The unpredictability and diversity of these events  
110 make structural interventions often inappropriate to reduce the related risk, and real-time  
111 monitoring network difficult to implement.

112 In the last decade, Wireless Sensor Networks (WSNs) have been largely used in various fields. A  
113 significant increase in the use of WSN, due to their simplicity, low cost of installation,  
114 manufacturing and maintenance, has been recorded in the framework of environmental monitoring  
115 applications (Intrieri et al., 2012; Liu et al., 2007; Yoo et al., 2007). Distinct types of sensor nodes  
116 of these networks, distributed with high density in the monitored areas, send environmental  
117 information to the concentrators nodes, generating a considerable amount and a wide variety of  
118 collected data. Due to the significant growth of data volumes to be transferred, the WSN require

119 flexible ad-hoc protocols, able to respect constraints related to energy consumption management  
120 (Hadadian and Kavian, 2016; Khaday et al., 2015; Parthasarathy et al., 2015). In particular, many  
121 protocols have been developed that offer data aggregation patterns to optimize the sensor nodes  
122 battery life (Kim et al., 2015) or sleep/measurement/data transfer cycles to minimize the energy  
123 consumption (Fei et al., 2013; Venkateswaran and Kennedy, 2013).

124 LEWIS (Costanzo et al., 2016) uses heterogeneous sensors, distributed in the risk areas, to monitor  
125 the several physical quantities related to landslides. The measured data, through a  
126 telecommunications network, flow into the Data Collecting and Processing Center (DCPC), where,  
127 using suitable mathematical models for the monitored site, the risk is evaluated and eventually the  
128 state of alert for mitigation action is released (Figure 1).

129 The system, through a modular architecture exploiting a telecommunication network (called  
130 LEWARnet) based on an ad-hoc communication protocol and an adaptive middleware, has a high  
131 flexibility, which allows for the use of different interchangeable technological solutions to monitor  
132 the parameters of interest.



133

134

**Figure 1. LEWIS architecture.**

135

136 The network has been equipped with both single point sensors as well as area sensors. The present  
137 paper addresses a sub-network comprising an area sensor, the GB-InSAR.

138 The different sensors types generate asynchronous traffic, thus imposing the adoption of an ad-hoc  
139 transmission protocol. This can support an asynchronous transmission mode to the DCPC, and it is

140 equipped with message queues management capacity to reconstruct historical data series, between  
141 two connection sessions, in case of null or partial transmission. This operation mode requires the  
142 presence of a software architecture that operates as a buffer, acting as an intermediary or as  
143 middleware (LEWARnet), between the data consumer (DCPC) and the data producers (sensors and  
144 sub-networks of sensors).

145 The developed middleware also monitors the processes of transmission and data acquisition,  
146 recognizing the activity status of the sensors and that of the DCPC, and integrating encryption and  
147 data compression functions.

148 A detail description of LEWIS can be found in Costanzo et al. (2015; 2016).

149

### 150 *3.3 Data Collecting and Processing Center*

151 The management of information flows, the telematic architecture and the services for data  
152 management are entrusted to the DCPC.

153 The DCPC has been designed and performed according to a complex hardware and software  
154 system, able to ensure the reliability and continuity of the service, providing advance information of  
155 possible dangerous situations that may occur.

156 In the research project, the DCPC has to ensure the continuous exchange of information among  
157 monitoring networks, mathematical models and the Command and Control Center (CCC), that is  
158 responsible for emergency management and decision making.

159 Data flow from the monitoring network was managed according to a communication protocol,  
160 implemented by the DCPC, and named AqSERV. AqSERV was designed considering the  
161 heterogeneity of devices of monitoring and transmission networks (single point and area sensors)  
162 and the available hardware resources (microcontrollers and/or industrial computers). AqSERV was  
163 devised to link DCPC database (named LEWISDB) to the monitoring networks, after validation for  
164 the authenticity of the node that connects to the center. Data acquisition, before the storage in the  
165 database, is validated both syntactically and according to the information content. The procedures  
166 for extraction of the information content and validation have been realized differently for single  
167 point and area sensors: the latter require a more complex validation, as they work in a 2D domain.

168 The complete management of the monitoring networks by DCPC has been realized through specific  
169 remote commands, sent to individual devices via AqSERV, to reconfigure the acquisition intervals  
170 or to activate any sensor, depending on the natural phenomena occurring in real time.

171 The configuration of monitoring networks, composed by devices and sensors, of communication  
172 protocol used by each network, and of rules for extraction and validation of information content is  
173 carried out through a web application that allows for the management of the entire system by the  
174 users.

175 The real-time search for acquisitions is carried out through a WebGIS, specifically designed for  
176 WSNs, but that can be easily extended to classic monitoring networks.

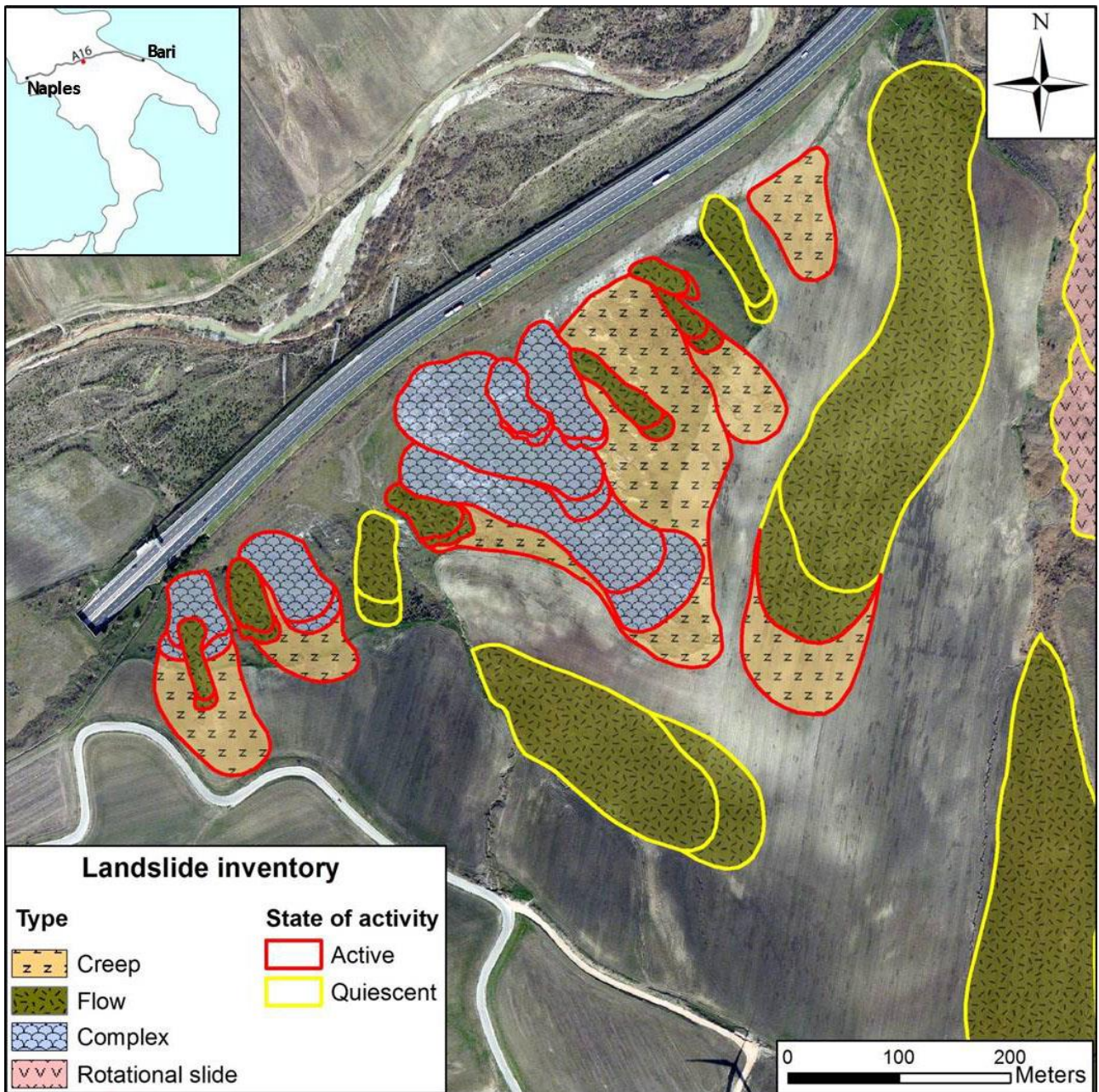
177 The WebGIS was designed according to the traditional web architecture, client-server, by using  
178 network services which are web mapping oriented:

- 179 - web server for static data;
- 180 - web server for dynamic data;
- 181 - server for maps;
- 182 - database for the management of map data.

183

184 **4 Test site**

185 The test site chosen to experiment the integrated system is located in Southern Italy, along a section  
186 of the A16 highway, an important communication route that connects Naples to Bari (Figure 2).  
187 The A16 selected section develops in SW-NE direction, along the Southern Italian Apennine, in  
188 correspondence with the valley of the Calaggio Creek, between the towns of Lacedonia (Campania  
189 Region) and Candela (Puglia Region).



190

191 **Figure 2. Landslides detected through field survey along the monitored section of A16 highway.**

192 The area is tectonically active, but the landscape, characterized by gentle slopes, is mostly  
193 influenced by lithologic factors rather than by tectonics. The lithologies outcropping in this area are

194 Pliocene-Quaternary clay, clayey marlstones, and more recent (Holocene) terraced alluvial  
195 sediments (from clay to gravel). The landslides shown in Figure 2 are all located in clay or clayey  
196 marlstones.

197 The highway runs on the right flank of the Calaggio Creek at an altitude between 300 and 400 m  
198 a.s.l.; the section of interest represents an element at risk in the computation of landslide risk  
199 assessment, due to the presence of unstable areas which can potentially affect the communication  
200 route (Figure 2). These unstable areas mainly involve clayey superficial layers.

201 On 1<sup>st</sup> July 2014, the GB-InSAR system was installed on the test site. The location of the  
202 installation point was selected taking into account the view of the unstable area and the distance  
203 from the power supply network. A covered structure was built to protect the system from  
204 atmospheric agents and possible acts of vandalism, in the perspective of a long-term monitoring.

205 The transmission network was provided by a GSM modem, exploiting the 3G network. In addition  
206 to the PC integrated in the GB-InSAR power base, a further external PC was exclusively employed  
207 for data post elaboration and transmission.

208 The system acquired from the beginning of July 2014 until the end of July 2015.

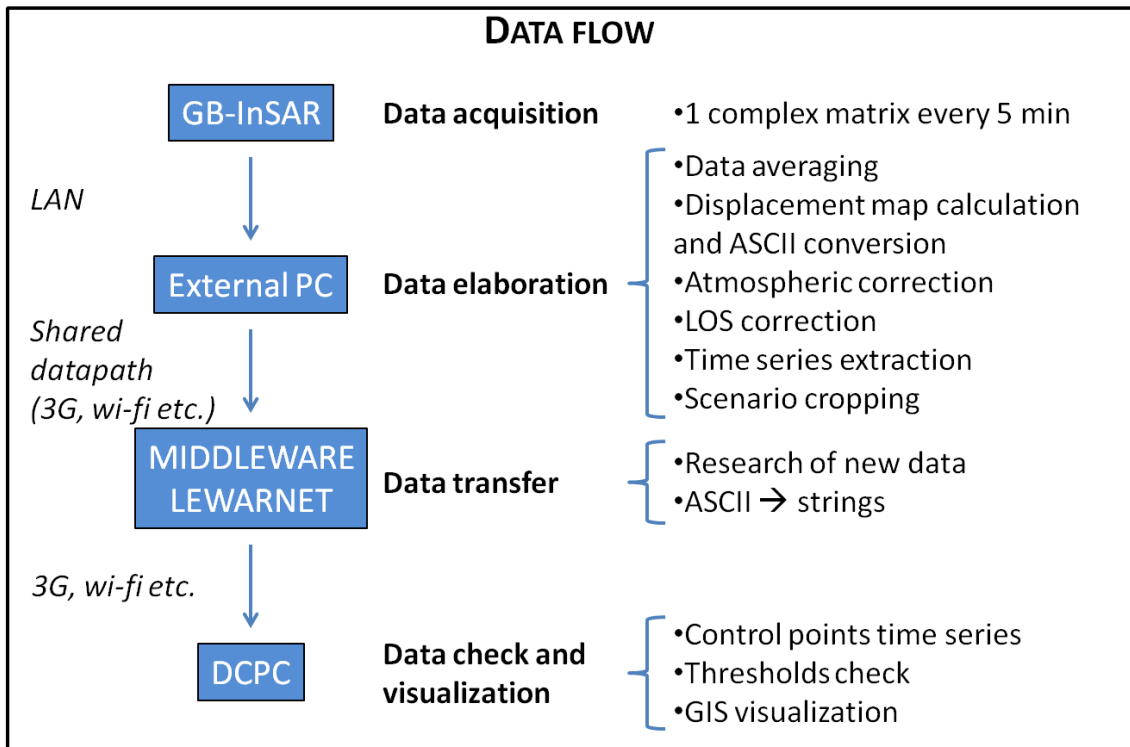
209 The installation location allowed the system to detect an area between 40 and 400 meters far from  
210 the its position in range direction, and about 360 m wide in the azimuth direction. These values,  
211 coupled with a 40° vertical aperture of the antennas, allowed operators to detect an area of about  
212 360 m x 360 m.

## 213 **5 Data management**

214 The most relevant matter of this monitoring was not as much related to the detection of landslide  
215 movements threatening the highway, as to how a long-term monitoring performed with an  
216 instrument providing huge amounts of data could have been run without resorting to large hard  
217 drives nor to fast internet connections. In fact, the monitoring area was covered by a 3G mobile  
218 telecommunication networks, with a limit of 2 gigabyte data transfer per month and there was the  
219 need to reduce the massive data flow produced by the radar.

220 For this reason, an appropriate data management (Figure 3) was developed and is here described.

221



222

223

**Figure 3. Diagram showing the complete data flow from acquisition to final visualization.**

224

### 5.1 Data acquisition

225

The GB-InSAR employed produced a single radar image, consisting in a 1001x1001 complex matrix, every 5 minutes. Each one is around 8 Megabytes large, resulting in more than 2 Gigabytes of data produced every day.

227

228

This amount of data represented an issue for both store capacity and data transmission.

229

### 5.2 Data elaboration

230

After being acquired, data were then transferred through LAN connection to the external PC implementing a dedicated Matlab script locally performing the actions described as follows.

231

232

#### 5.2.1 Data averaging

233

In order to reduce the noise normally affecting radar data (especially in vegetated areas), the images acquired every 5 minutes were also averaged using all data of the previous 8 and 24 hours. Then images averaged on 24 hours have been used to calculate daily displacement maps, every 8 hours to create 8h displacement maps and non-averaged images to calculate 5 minutes displacement maps. These time frames have been selected based on the characteristics of the slope movements and signal/noise ratio in the investigated area.

236

237

238

239

Averaging is also a mean to make a good use of a high data frequency, since it enables to reduce the memory occupied in the database as an alternative to their direct elimination.

240



241 5.2.2 Displacement map calculation and ASCII conversion

242 Each radar image can be represented as in Eq.1:

243 
$$S_n = A_n \exp(j\varphi_n) \tag{1}$$

244 where  $A_n$  is the amplitude of the  $n^{\text{th}}$  image,  $\varphi_n$  its phase and  $j = (-1)^{1/2}$  is the imaginary unit. The  
245 displacement  $\Delta r$  occurred in the time period between the acquisition of  $S_1$  and  $S_2$  has been  
246 calculated with the following (Eq.2):

247 
$$\Delta r = (\lambda/4\pi) \cdot \Delta\varphi \tag{2}$$

248 where  $\lambda$  is the wavelength of the signal and

249 
$$\Delta\varphi = \varphi_1 - \varphi_2 \tag{3}$$

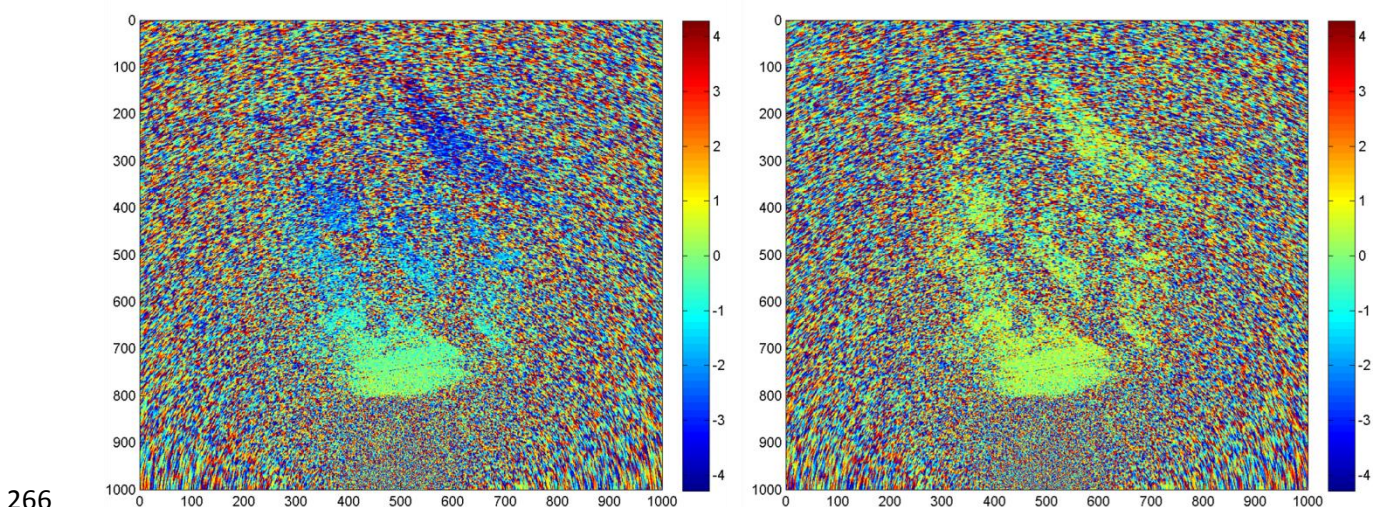
250 can be derived from:

251 
$$S_3 = S_1 S_2^* = A_1 A_2 \exp[j(\varphi_1 - \varphi_2)] \tag{4}$$

252 As a result, an ASCII file, only containing the information relative to the displacement for each  
253 pixel, was obtained.

254 5.2.3 Atmospheric correction

255 One of the major advantages of GB-InSAR is the capability to achieve sub-millimeter precision.  
256 However, this can be severely hampered by the variations of air temperature and humidity,  
257 especially when long distances are involved. Usually, atmospheric correction is performed by  
258 choosing one area considered stable, taking into account that every displacement value different  
259 from 0 is due to atmospheric noise and assuming that this offset is a linear function of the distance.  
260 Based on this relation all the displacement map is corrected. In our case the whole scenario has been  
261 selected and then only the potential unstable zones and those with a weak or incoherent  
262 backscattered signal were removed. The remaining areas were then considered stable and therefore  
263 were used for calculating the atmospheric effects. This results in a larger correction region that  
264 enables a statistical correlation between the atmospheric effects and the distance and therefore the  
265 calculation of a site-specific regression function that may not necessarily be linear (Figure 4).



267 **Figure 4. The color bar is expressed in mm; green indicates stable pixels, while blue and red**  
268 **respectively movement toward and away from the GB-InSAR. Left: raw interferogram showing**  
269 **artificial displacement increasing linearly with distance (as typical of atmospheric noise). Right: the**  
270 **same interferogram after the atmospheric correction.**

#### 271 5.2.4 Line of sight correction

272 The availability to detect only the Line Of Sight (LOS) component of the displacement vector  
273 represents one of the main limitations of the GB-InSAR technique. A method to partially overcome  
274 this limitation has been applied in this paper, following the procedure described in Colesanti and  
275 Wasowski, 2006 and later in Bardi et al. 2014, 2016. Other methods have been employed by  
276 Cascini et al. (2010; 2013).

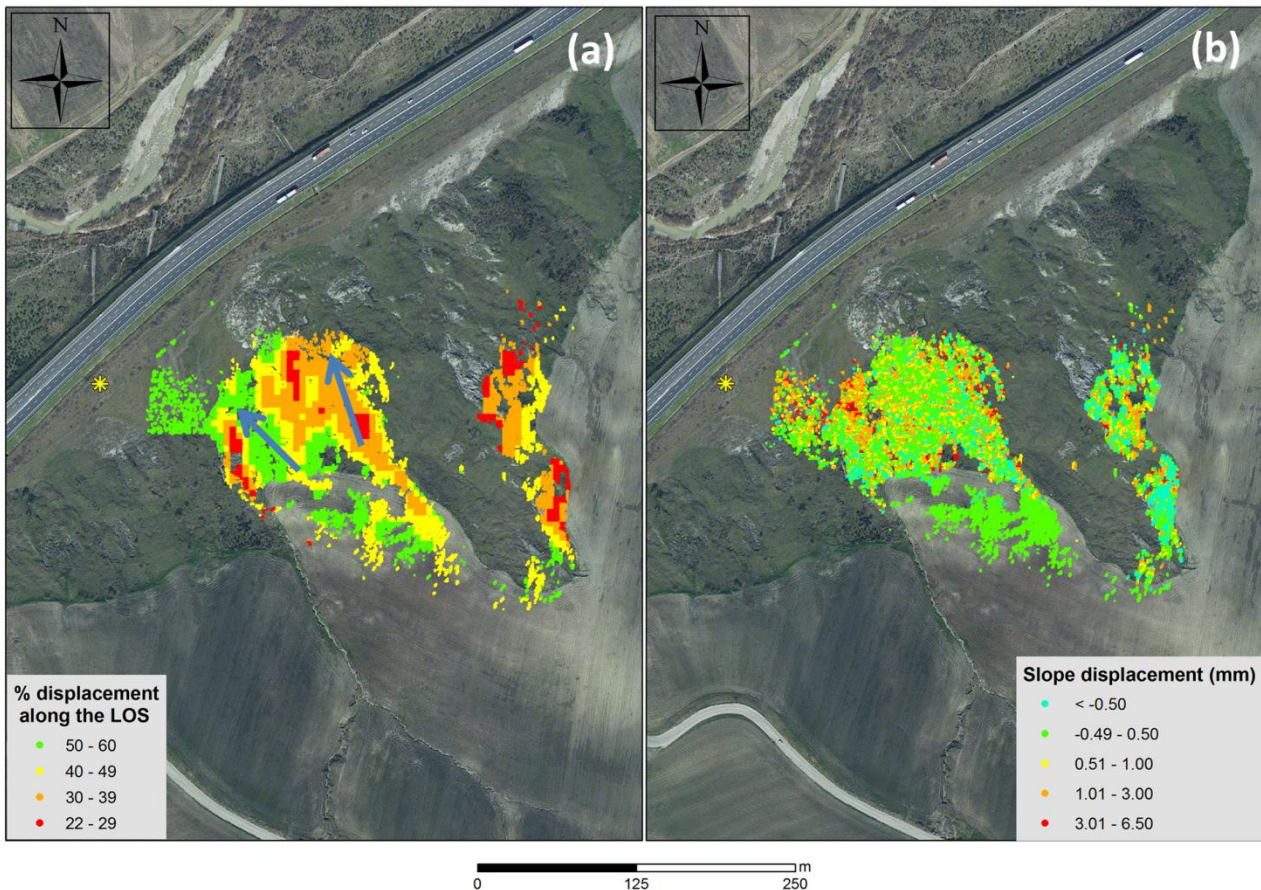
277 Assuming the downslope direction as the most probable displacement path, radar data have been  
278 projected on this direction. Input data as the angular values of *Aspect* and *Slope* have been derived  
279 from the *Digital Terrain Model* (DTM) of the investigated area; furthermore, azimuth angle and  
280 incidence angle of the radar LOS have been obtained.

281 After calculating the direction cosines of LOS and Slope (respectively functions of azimuth and  
282 incidence angles and aspect and slope angles) in the directions of Zenith ( $Z_{los}$ ,  $Z_{slope}$ ), North ( $N_{los}$ ,  
283  $N_{slope}$ ) and East ( $E_{los}$ ,  $E_{slope}$ ), the coefficient  $C$  is defined as follow (Eq. 5):

$$284 \quad C = Z_{los} \times Z_{slope} + N_{los} \times N_{slope} + E_{los} \times E_{slope} \quad (5)$$

285  $C$  represents the percentage of real displacement detected by the radar sensor (Figure 5A).

286 The real displacement ( $D_{real}$ ) is defined as the ratio between the displacement recorded along the  
287 LOS ( $D_{los}$ ) and the  $C$  value (Figure 5 B).



288

289 **Figure 5. (a) C values map. Blue arrows indicate the downslope direction. (b) Cumulated displacement**  
 290 **values projected along the downslope direction, referred to a period between 1 July 2014 and 1**  
 291 **November 2014. The yellow asterisk in the left of the images represents the location of the GB-InSAR.**

292 Assuming that the studied landslide actually moves along the downslope direction, the GB-InSAR  
 293 detectable real displacement percentage ranges between 22 and 60 % (Figure 5A).

294 In Figure 5B, an example of slope displacement map has been shown. Here, cumulated  
 295 displacement data related to a period between 1 July and 1 November 2014 have been projected  
 296 along the downslope direction. Data show as the area can be considered stable in the referred  
 297 period; maximum displacement values of 4 mm in 4 months (eastern portion of observed scenario)  
 298 can be still considered in the range of stability.

### 299 5.2.5 Time series extraction

300 In order to allow for a fast data transfer and velocity threshold comparison, some representative  
 301 control points were selected, aimed at providing cumulated displacement time series. Control points  
 302 were retrieved from the same displacement maps calculated as described in paragraph 5.2.2 and  
 303 therefore can be relative to a time frame of 5 minutes, 8 hours or 24 hours.

304 In case of noisy data, instead of having a time series relative to a single pixel, these can be retrieved  
 305 from a spatial average obtained from a small area consisting of few pixels.

## 306 5.2.6 Scenario cropping

307 Typically, the field of view of a GB-InSAR is larger than the actual area to be monitored. In fact, a  
308 portion of the radar image may be relative to the ground, sky, areas geometrically shadowed or  
309 covered by dense vegetation. These may be of no interest or even containing no information at all.  
310 For the case here studied around 50% of a radar image had a low coherence and was for all practical  
311 purposes, unusable. Therefore, a cropping of the ASCII displacement map occurred in order to  
312 frame only the relevant area.

## 313 5.3 *Data transfer and visualization*

314 The interferometric data generated by GB-InSAR, after the pre-processing and proper correction  
315 previously described, are ready for transfer to the DCPC. The transmission of these data to the  
316 DCPC is mediated by the middleware, which interrogates the GB-InSAR for tracking the state,  
317 detects the newest data, and reorders and marks them to properly build data time series to be  
318 transferred to DCPC.

319 Subsequently, the middleware manages communications with the DCPC, according to the  
320 implemented ad-hoc protocol. This ensures the security of data providers through encrypted  
321 authentication mechanisms, it allows for recovering missing or partially transmitted data, thus  
322 avoiding information loss, and provides data acquired by the sensors to the DCPC in a standardized  
323 format, JSON, able to guarantee uniformity between the various information provided by the  
324 various sensors types. All these particular features fully justify the adoption of an ad-hoc protocol  
325 for data transfer, instead of using a standard protocol such as FTP.

326 The data files produced by the GB-InSAR have already been locally pre-processed and result in a  
327 matrix expressed in ASCII code; the dimensions of the matrix are known and range from 1x1 (for  
328 the displacement of single control points) to 1001x1001 (for uncropped displacement maps). Before  
329 encapsulating these data in the message to be transferred to DCPC, the middleware converts them  
330 from ASCII code to character strings, using the standard coding ISO / IEC 8859-1, so being able to  
331 obtain a data compression with a factor equal to  $\approx 8$ .

332 Eventually the DCPC is entrusted for cumulating the displacements relative to the control points,  
333 which are compared with the respective thresholds, and for visualizing the displacement maps as  
334 WebGIS layers, thus enabling data validation and the evaluation of the extension of moving surface.

## 335 **6 Early warning procedures discussions**

336 The GB-InSAR is part of a larger early warning system (LEWIS) which also includes other  
337 monitoring systems and simulation models. Therefore, to understand how GB-InSAR data can be  
338 used in an early warning perspective, it is necessary to make reference to LEWIS as a whole.

339 Any information, coming from the investigated sites and subsequently processed also by using the  
340 simulation models, is used to define an intervention model. This is based on the following elements:  
341 event scenarios, risk scenarios, levels of criticality, levels of alert.

342 Event scenarios describe the properties of expected phenomena in terms of dimension, velocity,  
343 involved material and occurrence probability. Occurrence probability depends on the associated  
344 time horizon, which should be equal to few hours at most, in the case of early warning systems.

345 Evaluation of occurrence probability is carried out by using information from monitoring systems  
346 and/or from outputs of adopted mathematical models for nowcasting. All the properties, to be  
347 analyzed for event scenarios, are listed below; a subdivision in classes is adopted for each one:

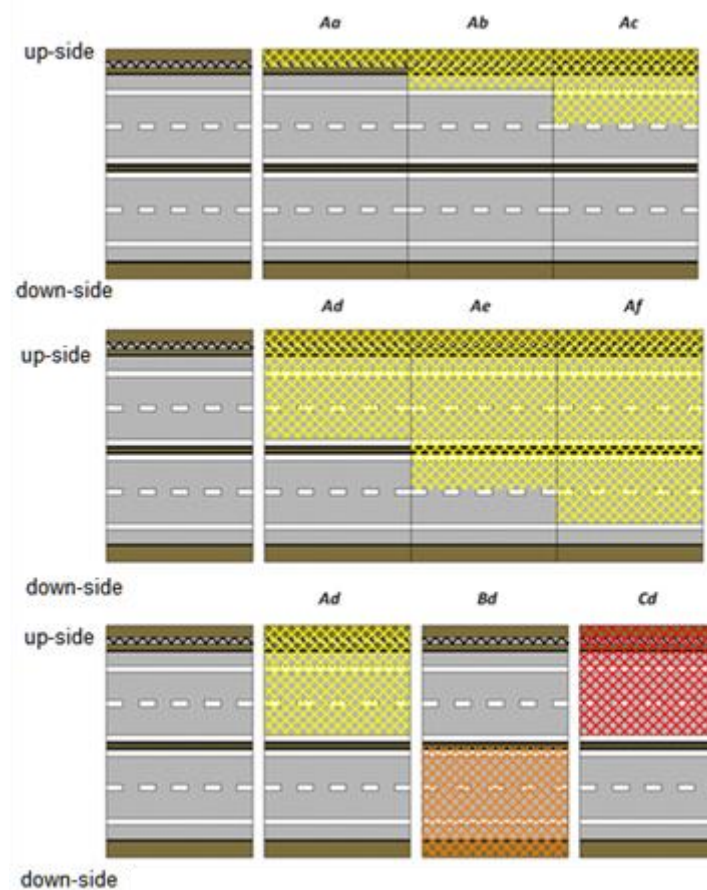
- 348 • landslide velocity (5 classes from slow to extremely rapid);
- 349 • landslide surface (5 classes from very small to very large);
- 350 • landslide scarp (5 classes from very small to very large);
- 351 • landslide volume (5 classes from extremely small to large);
- 352 • thickness (5 classes from very shallow to very deep);
- 353 • magnitude (3 classes: low, moderate, high), which combines the previous information;
- 354 • involved material (mud, debris, earth, rock, mixture of components);
- 355 • occurrence probability (zero, low, moderate, high, very high, equal to 1).

356 While some of the aforementioned parameters are determined by geological surveys, landslide  
357 velocity is directly derived from monitoring data (such as those collected by GB-InSAR). Landslide  
358 surface can be determined by geomorphological observation but is precisely quantified by GB-  
359 InSAR, thanks to its capability of producing 2D displacement maps.

360 Risk scenarios can be firstly grouped in the following three classes:

- 361 A. mud and/or debris movements which could induce a friction reduction between the vehicles  
362 and the tar and therefore facilitate slips;
- 363 B. road subsidence induced by landslides that could drag or drop vehicles;
- 364 C. falls of significant volumes and/or boulders that could crush or cover vehicles and constitute  
365 an obstacle for other vehicles.

366 For each previous risk scenario, six sub-scenarios can be identified based on the number of  
367 potentially involved infrastructures, carriageways and lanes (a. hydraulic infrastructures and/or  
368 barriers, b. only emergency lane, c. lane, d. fast lane, e. fast lane of the opposite carriageway, f. lane  
369 of the opposite carriageway). Thus, all possible risk scenarios are 18 (Figure 6), indicated with a  
370 couple of letters (Capital and small).



371  
 372 **Figure 6. Top and middle: possible risk scenarios involving the scenario A (landslides that could**  
 373 **reduce friction) to increasing sectors of the highway. Bottom: combinations of scenarios with several**  
 374 **types of phenomena (A, B, C) affect the emergency lane, lane and fast lane.**

375 The following information is provided to DCPC:

- 376 • Measurements from sensors
- 377 • Model outputs

378 and four states are identified for each of them:

- 379 • state 0 = no variation
- 380 • state 1 = small variation
- 381 • state 2 = moderate variation
- 382 • state 3 = high variation.

383 In practice, for the GB-InSAR, such states are delimited by fixed velocity values (thresholds). In  
 384 this application values have been selected according to the gathered data, the first threshold being  
 385 just above the instrumental noise; the remaining have been set based on expert judgement waiting  
 386 for a more robust calibration, which is possible only after at least a partial mobilization of the slope.  
 387 Anyway, the system is open to any method for determining thresholds (Crosta and Agliardi, 2003;  
 388 Du et al., 2013; Carlà et al., 2016a) and also to the use of other parameters (acceleration for  
 389 example).

390 Besides information from sensors and models, other information is obtained from meteorological  
 391 and hydrological models (named as indicators).

392 Indicators comprise weather forecasting and output of Forecasting of Landslides Induced by  
 393 Rainfall (FLaIR) and Saturated Unsaturated Simulation for Hillslope Instability (SUSHI) models

394 (Sirangelo et al. 2003; Capparelli and Versace 2011) on the basis of observed and predicted (for the  
 395 successive six hours) rainfall heights.

396 Two states are defined for indicators:

- 397 • state 0 = no variation or not significant,
- 398 • state 1 = significant variation.

399 To sum up, DCPC has the following information in any moment:

- 400 ▶ state (0, 1) of indicators (IND),
  - 401 ▶ state (0, 1, 2, 3) of sensors and models running for the specific highway section (SEN),
- 402 and, on the basis of these states, four different decisions can be made by DCPC, one of which with  
 403 three options.

404 All the possible decisions are illustrated in Table 1, in which the weight of the several sensors is  
 405 assumed to be the same. Based on the notices of criticality levels provided by the DCPC, and on its  
 406 own independent evaluations, the CCC issues the appropriate warning notices (Surveillance, Alert,  
 407 Alarm and Warning) and makes decisions about the consequent actions.

408

State of sensors and/or models	DCPC decisions
All INDs and SENs are S0	0 - no decision
At least one IND is S1 and all SENs are S0	1 – Sensor on demand activation
At least one SEN is S1	2 – to intensify the presence up to 24 hours/day
At least $n$ SENs are S1 or at least one SEN is S2	3/1 – to issue a notice of ordinary criticality (level 1)
At least $n$ SENs are S2 or at least one SEN is S3	3/2 - to issue a notice of moderate criticality (level 2)
At least $n$ SENs are S3	3/3 - to issue a notice of high or severe criticality (level 3)

409

**Table 1. DCPC possible decisions.**

410 The information of each sensor and the results produced by the models are used to assess, in each  
 411 instant, the occurrence probability of an event scenario in the monitored areas and the possible risk  
 412 scenarios.

413 This combination of heterogeneous data was carried out by identifying for each sensor and model a  
 414 typical information (displacement, precipitation, inclination, etc.), evaluating the state in each  
 415 instant, according to a threshold system, and combining this result for all sensors placed in a  
 416 monitored geomorphological area.

417 The result is constituted by the occurrence probability of an event scenario, that is associated with a  
 418 specific action by the DCPC. In particular, if the occurrence probability is low, moderate or high it  
 419 is necessary to issue a notice of criticality (ordinary - Level 1, moderate - Level 2, High - Level 3)  
 420 to the CCC.

421 The DCPC sends two types of information:

- 422 1) criticality state of the single monitored geomorphological unit,
- 423 2) criticality state of the whole area.

424 The adopted communication protocol between the two centers for the exchange of information was  
425 carried out through a web service provided by the CCC, using the classes and attributes of the  
426 methodology named Datex II (which is a protocol for the exchange of traffic data). The use of the  
427 web service allowed to ensure the interoperability of data between the two centers, regardless of the  
428 used hardware and software architecture, through a persistent service capable of ensuring an  
429 immediate restoration of the connections, in case of malfunction and a continuous monitoring  
430 between the two centers, even in the absence of criticality.  
431

## 432 **7 Conclusions**

433 The GB-InSAR is a monitoring tool that is becoming more and more used in landslide monitoring  
434 and early warning, especially thanks to its capability of producing real-time, 2D displacement maps.  
435 On the other hand, it still suffers from some drawbacks, such as the limitation of measuring only the  
436 LOS component of a target's movement and logistic issues like those owing to a massive  
437 production of data that may cause trouble for both storing capacity and data transfer. In particular,  
438 the latter is a more and more common problem of advanced technologies that are able to produce  
439 high quality data with a high acquisition frequency, which may leave the problem of find the  
440 balancing between exploiting all the information and at the same time avoiding unnecessary  
441 redundancy.

442 These problems have been addressed when a GB-InSAR was integrated within a complex early  
443 warning system (LEWIS) and only a limited internet connection was available. This situation  
444 required that a series of pre-elaboration processes and data management procedures took place in  
445 situ, in order to produce standardized and reduced files, carrying only the information needed when  
446 it was needed. The procedures mainly concerned the transmission of data averaged over determined  
447 time frames, proportionate with the kinematics of the monitored phenomenon. Previously,  
448 transmission data were also corrected (both in terms of atmospheric noise and LOS) and reduced,  
449 by filtering out the information relative to the amplitude of the targets, by eliminating the areas not  
450 relevant for the monitoring and by transforming the matrices into strings.

451 As a result, GB-InSAR data converged into the early warning system and contributed to it by  
452 producing displacement time series of representative control points to be compared with fixed  
453 thresholds. Displacement maps were also available for data validation by expert operators and for  
454 retrieving information relative to the surface of the moving areas.

455

456 *Competing interests.* The authors declare that they have no conflict of interest.

457

458 *Acknowledgements.* This research is part of the project “LEWIS (Landslides Early Warning  
459 Integrated System): An Integrated System for Landslide Monitoring, Early Warning and Risk  
460 Mitigation along Lifelines”, financed by the Italian Ministry of Education, Universities and  
461 Research and co-funded by the European Regional Development Fund, in the framework of the  
462 National Operational Programme 2007-13 “Research and Competitiveness”, grant agreement no.  
463 PON01\_01503.



464 The Authors are thankful to Giuseppe Della Porta and his colleagues from Autostrade S.p.A. for  
465 their availability in permitting and supporting the installation and maintenance of the GB-InSAR  
466 along the A16 highway.

## 467 **References**

- 468 Antonello, G., Casagli, N., Farina, P., Leva, D., Nico, G., Sieber, A. J. and Tarchi, D.: Ground-  
469 based SAR interferometry for monitoring mass movements. *Landslides*, 1 (1), 21-28, 2004.
- 470 Baldrige, S.M. and Marshall, J.D.: Performance of structures in the January 2010 MW 7.0 Haiti  
471 earthquake. In: *Structures Congress*, 2011. doi: 10.1061/41171(401)145.
- 472 Bamler, R. and Hartl, P.: Synthetic Aperture Radar Interferometry. *Inverse Probl*, 14, R1-R54,  
473 1998.
- 474 Bardi, F., Frodella, W., Ciampalini, A., Del Ventisette, C., Gigli, G., Fanti, R., Basile, G., Moretti,  
475 S. and Casagli, N.: Integration between ground based and satellite SAR data in landslide mapping:  
476 The San Fratello case study”, *Geomorphology*, 223, 45-60, 2014.
- 477 Bardi, F., Raspini, F., Ciampalini, A., Kristensen, L., Rouyet, L., Lauknes, T. R., Frauenfelder, R.  
478 and Casagli, N.: Space-Borne and Ground-Based InSAR Data Integration: The Åknes Test Site.  
479 *Remote Sens-Basel*, 8(3), 237, 2016.
- 480 Bardi, F., Raspini, F., Frodella, W., Lombardi, L., Nocentini, M., Gigli, G., Morelli, S., Corsini, A.  
481 and Casagli, N.: Monitoring the Rapid-Moving reactivation of Earth Flows by Means of GB-  
482 InSAR: The April 2013 Capriglio Landslide (Northern Apennines, Italy). *Remote Sens-Basel*, 9(2),  
483 165, 2017.
- 484 Cagno, E., De Ambroggi, M., Grande, O. and Trucco, T.: Risk analysis of underground  
485 infrastructures in urban areas. *Reliab Eng Syst Safe* 96, 139-148, 2011.
- 486 Calvari, S., Intrieri, E., Di Traglia, F., Bonaccorso, A., Casagli, N. and Cristaldi, A.: Monitoring  
487 crater-wall collapse at active volcanoes: a study of the 12 January 2013 event at Stromboli. *B*  
488 *Volcanol*, 78 (5), 39, 2016.
- 489 Capparelli, G. and Versace, P.: FLAIR and SUSHI: Two mathematical models for early warning of  
490 landslides induced by rainfall. *Landslides*, 8 (1), 67-79, 2011.
- 491 Carlà, T., Intrieri, E., Di Traglia, F. and Casagli, N.: A statistical-based approach for determining  
492 the intensity of unrest phases at Stromboli volcano (Southern Italy) using one-step-ahead forecasts  
493 of displacement time series. *Nat Hazards*, 84 (1), 669-683, 2016a.
- 494 Carlà, T., Intrieri, E., Di Traglia, F., Nolesini, T., Gigli, G. and Casagli, N.: Guidelines on the use of  
495 inverse velocity method as a tool for setting alarm thresholds and forecasting landslides and  
496 structure collapses. *Landslides*, 14(2), 517-534, 2016b.
- 497 Cascini, L., Fornaro, G. and Peduto, D.: Advanced low- and full-resolution DInSAR map  
498 generation for slowmoving landslide analysis at different scales. *Eng Geol*, 112 (1-4), 29-42,  
499 doi:10.1016/j.enggeo.2010.01.003, 2010.

500 Cascini, L., Peduto, D., Pisciotta, G., Arena, L., Ferlisi, S. and Fornaro, G.: The combination of  
501 DInSAR and facility damage data for the updating of slow-moving landslide inventory maps at  
502 medium scale. *Nat Hazard Earth Sys*, 13, 1527-1549, doi:10.5194/nhess-13-1527-2013, 2013.

503 Colesanti, C. and Wasowski, J.: Investigating landslides with space-borne Synthetic Aperture Radar  
504 (SAR) interferometry. *Eng Geol*, 88, 173–199, 2006.

505 Costanzo, S., Di Massa, G., Costanzo, A., Morrone, L., Raffo, A., Spadafora, F., Borgia, A.,  
506 Formetta, G., Capparelli, G. and Versace, P.: Low-cost radars integrated into a landslide early  
507 warning system. *Adv Intell Syst*, 354, 11-19, 2015.

508 Costanzo, S., Di Massa, G., Costanzo, A., Borgia, A., Raffo, A., Viggiani, G. and Versace, P.:  
509 Software-defined radar system for landslides monitoring. *Adv Intell Syst*, 445, 325-331, 2016.

510 Crosta, G.B. and Agliardi, F.: How to obtain alert velocity thresholds for large rockslides. *Phys*  
511 *Chem Earth, Pt A/B/C*, 27 (36), 1557-1565, 2002.

512 Del Ventisette, C., Intrieri, E., Luzi, G., Casagli, N., Fanti, R. and Leva, D.: Using ground based  
513 radar interferometry during emergency: The case of the A3 motorway (Calabria Region, Italy)  
514 threatened by a landslide. *Nat Hazard Earth Sys*, 11 (9), 2483-2495, 2011.

515 Di Traglia, F., Nolesini, T., Intrieri, E., Mugnai, F., Leva, D., Rosi, M. and Casagli N.: Review of  
516 ten years of volcano deformations recorded by the ground-based InSAR monitoring system at  
517 Stromboli volcano: a tool to mitigate volcano flank dynamics and intense volcanic activity. *Earth-*  
518 *Sci Rev*, 139, 317-335, 2014.

519 Du, J., Yin, K. and Lacasse, S.: Displacement prediction in colluvial landslides, three Gorges  
520 reservoir, China. *Landslides*, 10 (2), 203-218, 2013

521 Fei, X., Zheng, Q., Tang, T., Wang, Y., Wang, P., Liu, W. and Yang H.: A reliable transfer protocol  
522 for multi-parameter data collecting in wireless sensor networks", 2013 15<sup>th</sup> Int Conf Adv Commun:  
523 Smart Services with Internet of Things, ICACT 2013, 569-573, 2013.

524 Geertsema, M., Schwab, J.W., Blais-Stevens, A. and Sakals, M.E.: Landslides impacting linear  
525 infrastructure in west central British Columbia. *Nat Hazards*, 48, 59-72, 2009.

526 Gene Corley, W., Mlakar, P.F.Sr., Sozen, M.A. and Thornton, C.H.: The Oklahoma City bombing:  
527 Summary and recommendations for multihazard mitigation. *J Perform Constr Fac*, 12, 100-112,  
528 1998.

529 Hadadian, H. and Kavian, Y.: Cross-layer protocol using contention mechanism for supporting big  
530 data in wireless sensor network", 2016 10<sup>th</sup> International Symposium on Communication Systems,  
531 Networks and Digital Signal Processing (CSNDSP), 2016.

532 Intrieri, E., Gigli, G., Mugnai, F., Fanti, R. and Casagli, N.: Design and implementation of a  
533 landslide early warning system. *Eng Geol*, 147-148, 124-136, 2012.

534 Intrieri, E., Gigli, G., Casagli, N. and Nadim, F.: Brief communication Landslide Early Warning  
535 System: Toolbox and general concepts. *Nat Hazard Earth Sys*, 13 (1), pp. 85-90, 2013.

536 Intrieri, E., Gigli, G., Nocentini, M., Lombardi, L., Mugnai, F. and Casagli, N.: Sinkhole  
537 monitoring and early warning: An experimental and successful GB-InSAR application.  
538 *Geomorphology*, 241, 304-314, 2015.

539 Kadri, F., Birregah, B. and Châtelet, E.: The impact of natural disasters on critical infrastructures: A  
540 domino effect-based study. *J Homel Secur Emerg*, 11, 217-241, 2014.

541 Khaday, B., Matson, E. T., Springer, J., Kwon, Y.K., Kim, H., Kim, S., Kenzhebalin, D., Sukyeong,  
542 C., Yoon, J. and Woo, H. S.: Wireless Sensor Network and Big Data in Cooperative Fire Security  
543 system using HARMS, 2015 6<sup>th</sup> International Conference on Automation, Robotics and  
544 Applications (ICARA), 2015.

545 Kim, Y., Bae, P., Han, J. and Ko, Y.B.: Data aggregation in precision agriculture for low-power and  
546 lossy networks", 2015 IEEE Pacif, 2015.

547 Kröger, W.: Critical infrastructures at risk: A need for a new conceptual approach and extended  
548 analytical tool. *Reliab Eng Syst Safe*, 93, 1781-1787, 2008.

549 Labaka, L., Hernantes, J. and Sarriegi, J.M.: A holistic framework for building critical infrastructure  
550 resilience. *Technol Forecast Soc*, 103, 21-33, 2016.

551 Liu, H., Meng, Z. and Cui S.: A Wireless Sensor Network Prototype for Environmental Monitoring  
552 in Greenhouses", 2007 Int C Wirel Comm Net, 2007.

553 Lombardi, L., Nocentini, M., Frodella, W., Nolesini, T., Bardi, F., Intrieri, E., Carlà, T., Solari, L.,  
554 Dotta, G., Ferrigno, F. and Casagli, N.: The Calatabiano landslide (southern Italy): preliminary GB-  
555 InSAR monitoring data and remote 3D mapping. *Landslides*, 1-12, 2016.

556 Luzi G.: Ground Based SAR Interferometry: a novel tool for geoscience. P. Imperatore, D. Riccio  
557 (Eds.), *Geoscience and Remote Sensing. New Achievements*, InTech, 1-26, 2010. (Available at:  
558 <http://www.intechopen.com/articles/show/title/ground-based-sar-interferometry-a-novel-tool-for-geoscience>).  
559 geoscience).

560 Martino, S. and Mazzanti, P.: Integrating geomechanical surveys and remote sensing for sea cliff  
561 slope stability analysis: The Mt. Pucci case study (Italy). *Nat Hazard Earth Sys*, 14 (4), 831-848,  
562 2014.

563 Monserrat, O., Crosetto, M. and Luzi, G.: A review of ground-based SAR interferometry for  
564 deformation measurement. *ISPRS J Photogramm*, 93, 40-48, 2014,

565 Parthasarathy, A., Chaturvedi, A., Kokane, S., Warty, C. and Nema, S.: Transmission of big data  
566 over MANETs. *Aerosp Conf Proc*, 2015.

567 Rudolf, H., Leva, D., Tarchi, D. and Sieber, A.J.: A mobile and versatile SAR system. *IGARSS*  
568 *Proc*, Hamburh, 1999.

569 Severin, J., Eberhardt, E., Leoni, L. and Fortin, S.: Development and application of a pseudo-3D pit  
570 slope displacement map derived from ground-based radar. *Eng Geol*, 181, 202-211, 2014.

571 Sirangelo, B., Versace, P. and Capparelli, G.: Forewarning model for landslides triggered by rainfall  
572 based on the analysis of historical data file. *IAHS-AISH P*, 278, 298-304, 2003.

573 Snyder, L. and Burns, A.A.: Framework for critical infrastructure resilience analysis. *Energy and*  
574 *systems analysis-infrastructure*. Sandia National Laboratories, 2009

575 Tapete, D., Casagli, N., Luzi, G., Fanti, R., Gigli, G. and Leva D.: Integrating radar and laser-based  
576 remote sensing techniques for monitoring structural deformation of archaeological monuments. *J*  
577 *Archaeol Sci*, 40(1), 176-189, 2013.

578 Tarchi, D., Ohlmer and E., Sieber, A.J.: Monitoring of structural changes by radar interferometry.  
579 Res Nondestruct Eval, 9, 213-225, 1997.

580 Tarchi, D., Rudolf, H., Luzi, G., Chiarantini, L., Coppo, P. and Sieber, A. J.: SAR interferometry  
581 for structural change detection: a demonstration test on a dam. Int Geosci Remote Se, 3, 1525-1527,  
582 1999.

583 Tarchi, D., Casagli, N., Fanti, R., Leva, D., Luzi, G., Pasuto, A., Pieraccini, M. and Silvano, S.:  
584 Landslide monitoring by using ground-based SAR interferometry: an example of application to the  
585 Tessina landslide in Italy. Eng Geol, 1, 68, 15-30, 2003.

586 Urlainis, A., Shohet, I.M., Levy, R., Ornai, D. and Vilnay, O.: Damage in critical infrastructures  
587 due to natural and man-made extreme Events – A critical review. Procedia Engineer, 85, 529-535,  
588 2014.

589 Urlainis, A., Shohet, I.M. and Levy, R.: Probabilistic Risk Assessment of Oil and Gas  
590 Infrastructures for Seismic Extreme Events. Procedia Engineer, 123, 590-598, 2015.

591 Venkateswaran, V. and Kennedy, I.: How to sleep, control and transfer data in an energy  
592 constrained wireless sensor network. 51<sup>st</sup> Annual Allerton Conference on Communication, Control,  
593 and Computing (Allerton), 2013.

594 Versace, P., Capparelli, G., Leone, S., Artese, G., Costanzo, S., Corsonello, P., Di Massa, G.,  
595 Mendicino, G., Maletta, D., Muto, F., Senatore, A., Troncone, A., Conte, E. and Galletta, D.:  
596 LEWIS project: An integrated system of monitoring, early warning and mitigation of landslides  
597 risk. Rendiconti Online Società Geologica Italiana, 21(1), 586-587, 2012.

598 Yoo, S., Kim, J., Kim, T., Ahn, S., Sung, J. and Kim, D.: A2S: Automated Agriculture System  
599 based on WSN. I Symp Consum Electr, 2007.